Research Article - Part of the Special Issue on Mechanics of Advanced Fiber-Reinforced Composite Structures

Stacking-Sequence Optimization and Buckling Analysis of Graphene/Fiber-Reinforced Laminated Plates

Ranganai Tawanda Moyo [a] * [iD], Pavel Yaroslavovich Tabakov [b]

[a] Department of Mechanical Engineering, Durban University of Technology, Durban, 4001, South Africa

[b] Department of Mechanical Engineering and Institute for Systems Science, Durban University of Technology, Durban, 4001, South Africa

ARTICLE INFO

ABSTRACT

The use of graphene-based composites, particularly in aerospace and structural applications, has received extensive attention in recent years. Graphene nanoplatelets are normally used to enhance composite materials' mechanical, thermal, and electrical properties. The present research investigates the biaxial buckling of two- and three-phase angle ply laminated plates reinforced with carbon or glass fibers. The simply supported plate in this study is defined as a 16-ply symmetric and balanced laminate with uniform distribution of the fiber and graphene content through the thickness. The objective of this work is to produce a cost-effective design using the minimum amount of expensive reinforcement while maximizing the compressive buckling load. The desired results are achieved by finding the optimal stacking sequence of reinforcement fibers, as well as selecting an optimal amount of graphene nanoplatelets and fiber volume content. Numerical results are first obtained for two-phase laminates with different ratios of applied loads. Further, three-phase laminates are studied and, among other things, the relationship between the fiber and graphene content is analyzed. The optimization procedures were performed by particle swarm optimization (PSO) for continuous optimization and genetic algorithm (GA) for integer optimization. The software applications were written by the authors and proved to be very fast and efficient.

1. Introduction

The importance of composite materials nowadays cannot be overestimated. They combine properties such as strength and lightweight. Composite materials can be tailored to suit specific requirements, offering a range of mechanical, thermal, and electrical properties based on the materials used. Composite materials are fabricated using various methods, each tailored to specific applications and material requirements Common methods include hand lay-up and spray-up for simple, low-cost parts; resin transfer molding (RTM) and vacuum bagging for more complex shapes with better fiber-to-resin ratios; autoclave processing for high-performance aerospace components; filament winding for cylindrical and long, continuous parts; and compression molding and injection molding for high-volume production. A comprehensive description of the science and engineering of short fiber-reinforced polymer composites can be found in [1] which summarizes the advances and developments in this area, and serves as a key reference for readers interested in entering this exciting field. With the advance of technology, composite materials can be further improved by

incorporating nano-inclusions, such as carbon nanotubes (CNTs), nano-clays, or graphene nanoplatelets (GNPs), into the matrix phase of a standard composite material leading to enhanced properties and novel functionalities. Such composites are called multiscale composites and combine three components, fibers, nano-inclusions, and elastic matrix [2, 3]. Among various nano-inclusions, GNPs stand out as the best nano-reinforcing filler in polymer composites due to their superior mechanical, thermal, and electrical properties. These nanoplatelets can significantly enhance polymer composites' mechanical strength, stiffness, and durability through enhanced interfacial bonding, and load transfer efficiency. For example, Rafiee, et al. [4] experimentally discovered that epoxy composites reinforced by GNPs can achieve a 31% increase in Young's modulus, and only a 3% increase is achieved when reinforced with the same amount of CNTs.

Further studies that prove that a small amount of GNPs significantly improves the mechanical properties of polymer composites can be found in [5-8]. The works mentioned above are useful for understanding the constitutive and material properties of GNP-reinforced composites; however, the ultimate goal of developing these advanced nanocomposites is their usage in practical engineering applications. In general, GNP-reinforced composites can be practically utilized as structural beams, plates, panels, or shells. The present study focuses on the design of GNP/fiber-reinforced laminated plates for maximizing the compressive buckling load. The problem of buckling and post-buckling in multilayer graphene-reinforced composite plates may be found in [9-11] while vibration analysis of multiscale composite plates is studied in [12-14]. The main problem with thin-walled composites or other structures is their tendency to buckle under compressive loads. Buckling is a critical failure mode that results in a sudden and often catastrophic deformation. The resistance of a structure to buckling depends on various factors, including the material properties, geometric configuration, and loading conditions. Enhancing the buckling resistance of GNP/fiber-reinforced laminated plates ensures their structural integrity and reliability in practical applications.

The design of laminated plates for maximum buckling load gained popularity in the second half of the 20th century [15-20]. Since then, several techniques have been developed and suggested for optimizing the buckling resistance of these plates. In the early stages, classical and analytical methods such as the classical lamination theory (CLT) [21, 22], and the Rayleigh-Ritz method [23, 24] were used to predict the buckling behavior of laminated composite plates. Although these methods are easy to implement, they are limited to simple geometries and boundary conditions [25]. Later on, the advent of finite element analysis (FEA) revolutionized buckling analysis, allowing for the examination of complex geometries and loading conditions. Linear buckling analysis, which involves solving the eigenvalue problem to find critical buckling loads, became widely used. However, FEA for buckling optimization of laminated composites is limited by the complexity of accurately modeling anisotropic and heterogeneous material properties, geometric and boundary conditions, and the need for fine meshes, which increase computational demand [26]. More recently, with the advent of evolutionary computation, several evolutionary algorithms have been developed and suggested as an alternative to classical and analytical methods. Evolutionary optimization techniques have since proved effective for the buckling optimization of laminated composite plates because of their ability to solve complex, multi-objective, and non-linear problems. However, most of the studies that employ evolutionary algorithms for buckling optimization of laminated plates focus on composite plates (two-phase) as given in [27-30] and only a few studies explored the application of evolutionary algorithms to optimize nanocomposite plates (three-phase) such as GNP/fiber-reinforced laminated plates. Thus, the present study extends the scope of buckling optimization by considering multi-scale, GNP/fiber-reinforced laminated plates using particle swarm optimization (PSO) and the genetic algorithm (GA). The objective of the study is to produce cost-effective designs using the minimum amount of expensive reinforcements while maximizing the compressive buckling load.

2. Design Variables for Buckling Analysis of Laminated Composite and Nanocomposite Plates

Buckling analysis of laminated composite and nanocomposite (LCNC) plates is a critical area of research, driven by the need to understand and predict the structural stability and load-carrying capacity of these materials in various engineering applications. The analysis process involves a comprehensive understanding and evaluation of several design variables, broadly categorized into geometric, material, and layup parameters.

Geometric variables play a significant role in determining the buckling behavior of LCNC. Research by Leissa [31] established the fundamental influence of plate dimensions (length, width, and thickness) on buckling performance. Length and width are directly

proportional to the critical buckling load, while the thickness has a more complex, often cubic relationship with buckling resistance. Boundary conditions, such as simply supported, clamped, and free edges, have been shown to affect the buckling load significantly. Studies by Baba [32] have demonstrated that clamped edges provide higher buckling resistance when compared to simply supported or free edges. The aspect ratio, defined as the ratio of length to width, is another critical geometric variable. Higher aspect ratios generally lead to lower critical buckling loads, affecting the stiffness and stability of plates [33].

Material variables are equally crucial, as the inherent properties (matrix & fiber contents) of LCNC plates dictate their mechanical response. Material Young's modulus, shear modulus, Poisson's ratio, and density are key parameters influencing the buckling characteristics. Soden, et al. [34] provided a detailed examination of how these material properties affect the performance of composite laminates. The selection of materials with high stiffness-to-weight ratios is particularly beneficial in enhancing buckling resistance, as demonstrated in studies by Chao, et al. [15], Ren [35], Aslan, and Şahin [36].

Layup variables are unique to LCNC plates and significantly influence their buckling behavior. The fiber orientation of each ply, often specified in angles like 0°, 45°, and 90°, and the stacking sequence determines the directional stiffness and strength of the laminate. The stacking sequence is considered the best design variable for buckling optimization and analysis of LCNC plates. The studies [37, 38] argue that the stacking sequence of layers in a laminate significantly affects its mechanical properties, including stiffness, strength, and stability. In these studies, it was demonstrated that different orientations and sequences of the plies can alter the overall behavior of the laminate, impacting its buckling resistance. Therefore, by optimizing the stacking sequence, engineers can tailor the laminate's properties to achieve the best performance under buckling loads.

Additionally, the studies [39-41] state that a balanced and symmetric layup tends to enhance buckling resistance, as it provides uniform stiffness and minimizes warping. Thus, this allows for precise control over the mechanical response, ensuring that the laminate can withstand higher loads before buckling occurs. The present research employs the stacking sequence as the main design variable for the buckling analysis and optimization of GNP/fiber-reinforced laminated plates due to the above-mentioned advantages.

3. Theoretical Formulation

3.1. Analysis and Theoretical Formulation

The analysis of buckling in laminated composite plates has been thoroughly studied and a large number of literary sources can be found. It involves studying the behavior of thin plates made up of multiple layers of different materials, which are bonded together. Buckling analysis typically starts with classical plate theory (CPT) which simplifies the 3D elastic behavior of composite plates into a 2D problem. The CPT assumes small deformations, and straight normals, and neglects transverse shear deformation, making it suitable for thin plates. The theory utilizes equilibrium equations, constitutive relations, and kinematic relations to derive the stiffness matrices (A, B, D), which describe the laminate's response to in-plane forces and out-of-plane moments. A simply supported plate subjected to biaxial compressive load is shown in Figure 1.

The loads per unit length in the x and y directions are λN_x and λN_y where λ is a variable amplitude parameter. The load per unit length N_x in the x direction is assumed to be equal to 1.0 units. The laminate is made of an even number of layers of the constant thickness t. Besides, for each θ-deg ply, there is $-\theta$-deg ply (angle-ply laminates). Such an arrangement of the plies ensures that the plate is symmetrical and balanced.
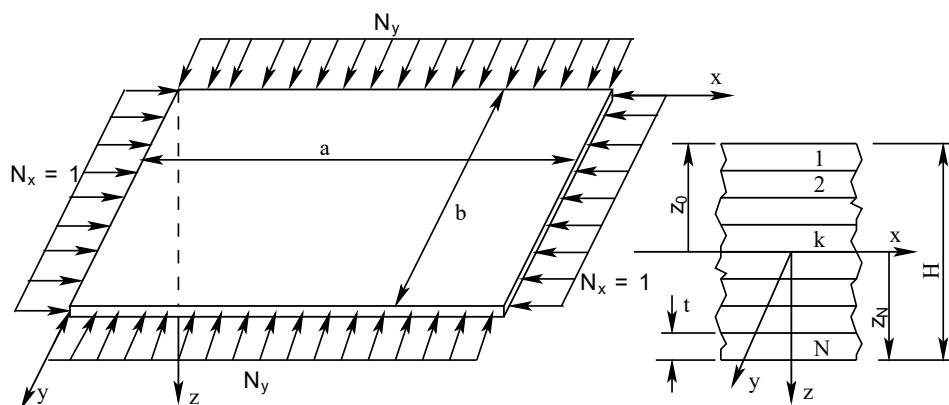
Fig. 1. Geometry and compressive loads of laminated rectangular plate

The buckling load of the angle-ply laminate is a well-known equation, given by equation (1). The plate buckles when the load amplitude λ reaches its critical value λ_{cr}. The optimization is performed over m and n, which are the numbers of half waves in the x and y directions, respectively.

$$\lambda_{cr}(m,n) = \frac{D_{11}\alpha_m^4 + 2(D_{12} + 2D_{66})\alpha_m^2\beta_n^2 + D_{22}\beta_n^4}{\alpha_m^2 + (N_y/N_x)\beta_n^2} \quad (1)$$

where $\alpha_m = \frac{\pi m}{a}$ and $\beta_n = \frac{\pi n}{b}$.

The flexural stiffnesses D_{ij} $(i, j = 1,2,6)$ in the above equation depend on the stacking sequence and are calculated as follows,

$$D_{ij} = \frac{1}{3}\sum_{k=1}^{N}\bar{Q}_{ij}^{(k)}(z_k^3 - z_{k-1}^3) \quad (2)$$

The transformed reduced stiffness coefficients $\bar{Q}_{ij}$ depend on the fiber orientation angle and are computed as

$$\bar{Q}_{11} = Q_{11}c^4 + 2(Q_{12} + 2Q_{66})c^2s^2 + Q_{22}s^4$$

$$\bar{Q}_{12} = (Q_{11} + Q_{22} - 4Q_{66})c^2s^2 + Q_{12}(c^4 + s^4)$$

$$\bar{Q}_{22} = Q_{11}s^4 + 2(Q_{12} + 2Q_{66})c^2s^2 + Q_{22}c^4 \quad (3)$$

$$\bar{Q}_{66} = (Q_{11} + Q_{22} - 2Q_{12} - 2Q_{66})c^2s^2 + Q_{66}(c^4 + s^4)$$

where $c = \cos\theta$ and $s = \sin\theta$. The elastic constants Q_{ij} are well-known expressions from the theory of elasticity.

$$Q_{11} = \frac{E_{11}}{\Delta_p}, \quad Q_{12} = \frac{\nu_{12}E_{22}}{\Delta_p}, \quad Q_{22} = \frac{E_{22}}{\Delta_p}, \quad Q_{66} = G_{12}$$

and $\Delta_p = 1 - \nu_{12}\nu_{21}$.

It is convenient to use the flexural stiffnesses and loads in terms of non-dimensional values [5], *viz*,

$$D_{ij0} = \frac{1.5D_{ij}}{E_{11}H^3} \quad (i,j = 1,2,6),$$

$$N_{x0} = \frac{1.5N_xa^2}{E_{11}H^3}, \quad N_{y0} = \frac{1.5N_ya^2}{E_{11}H^3}$$

Then, the non-dimensional critical buckling value can be rewritten as follows

$$\lambda_{cr}(m,n) = \frac{D_{110}m^4 + 2(D_{120} + 2D_{660})m^2n^2r^2 + D_{220}n^4r^4}{m^2N_{x0} + n^2r^2N_{y0}}w$$

$$(4)$$

where $r = a/b$.

3.2. Micromechanical Modeling

Nanocomposite materials consisting of the polymer matrix, and nano-inclusions such as graphene nanoplatelets and fibers (carbon, glass, or others) are called multiscale composite materials. Material properties of nanocomposites are determined via a micromechanical approach. First, we analyze the graphene-reinforced matrix, then with the added fiber reinforcement to the graphene polymer matrix.

The evaluation of effective Young's modulus, Poisson's ratio, and shear modulus of the graphene-reinforced matrix is presented in several research works, e.g. [11].

$$E_{GM} = \left(\frac{3}{8}\frac{1 + \zeta_L\eta_LV_{GPL}}{1 - \eta_LV_{GPL}} + \frac{5}{8}\frac{1 + \zeta_W\eta_WV_{GPL}}{1 - \eta_WV_{GPL}}\right)\times E_M \quad (5)$$

here, the subscript *GM* denotes graphene platelets in a reinforced matrix, while *M* refers to an unreinforced polymer matrix. The following quantities are used in the above equation. V_{GPL} is the volume content of graphene nanoplatelets. The parameters ζ_L and ζ_W are given in terms of platelet dimensions, namely, length l_{GPL}, width w_{GPL}, and thickness h_{GPL}.

$$\zeta_L = 2\frac{l_{GPL}}{h_{GPL}}, \quad \zeta_W = 2\frac{w_{GPL}}{h_{GPL}}$$

Coefficients η_L and η_W in Eq. (5) depend on the elastic moduli of the graphene E_{GPL} and the matrix E_M and are determined as

$$\eta_L = \frac{\left(E_{GPL}/E_M\right) - 1}{\left(E_{GPL}/E_M\right) + \zeta_L}, \quad \eta_w = \frac{\left(E_{GPL}/E_M\right) - 1}{\left(E_{GPL}/E_M\right) + \zeta_W}$$

The volume fraction of graphene content V_{GPL} is convenient to obtain in terms of weight fraction W_{GPL} and given as

$$V_{GPL} = \frac{W_{GPL}}{W_{GPL} + \left(\frac{\rho_{GPL}}{\rho_M}\right)(1 - W_{GPL})} \quad (6)$$

where ρ_{GPL} is the mass density of graphene, and ρ_M is the mass density of the polymer matrix. Finally, Poisson's ratio and shear modulus can be written as

$$\nu_{GM} = \nu_{GPL}V_{GPL} + \nu_M(1 - V_{GPL}),$$

$$G_{GM} = \frac{E_{GM}}{2(1 + \nu_{GM})} \quad (7)$$

Next, the obtained quantities can be used to calculate the effective material properties of the graphene nanoplatelets and fiber-reinforced matrix. These expressions are taken from [11]. The resulting properties of the three-phase composite material are given by

$$E_{11} = E_{F11}V_F + E_{GM}(1 - V_F) \quad (8)$$

$$E_{22} = E_{GM}\left(\frac{E_{F22} + E_{GM} + (E_{F22} - E_{GM})V_F}{E_{F22} + E_{GM} - (E_{F22} - E_{GM})V_F}\right) \quad (9)$$

$$G_{12} = G_{GM}\left(\frac{G_{F12} + G_{GM} + (G_{F12} - G_{GM})V_F}{G_{F12} + G_{GM} - (G_{F12} - G_{GM})V_F}\right) \quad (10)$$

$$\nu_{12} = \nu_{F12}V_F + \nu_{GM}(1 - V_F) \qquad (11)$$

where V_F is the fiber volume content and subscripts F11, F22, and F12 denote the material properties of the fibers.

4. GA and PSO Implementation

Particle swarm optimization and genetic algorithms are well-suited for optimizing the stacking sequence and analyzing the buckling of graphene/fiber-reinforced laminated plates due to their strengths in handling complex, nonlinear, and combinatorial optimization problems. Both methods excel in exploring large search spaces and maintaining solution diversity, which is crucial for stacking-sequence optimization's nonlinear and combinatorial nature. PSO's global search capability, adaptability, and GA's effective diversity maintenance through crossover and mutation make them robust for finding optimal solutions. Additionally, both methods can handle multiple objectives and constraints, making them ideal for optimizing composite materials' mechanical properties, weight, and cost.

4.1. Genetic Algorithms

- Problem formulation

To implement a GA for the stacking-sequence optimization and analysis of buckling in graphene/fiber-reinforced laminated plates, the first step involves defining the problem. The objective function is to maximize the buckling load while using the minimum amount of expensive nano-reinforcements. The main design variable is the stacking sequence, but other variables such as the weight fraction of GNPs and the volume content of carbon/glass fibers are also considered. After that, the next step is to initialize the population.

- Initial Population

The initial population is crucial for the GA's performance. Each individual in the population, represented as a chromosome, encodes a potential stacking sequence. This sequence can be represented in various ways, such as binary or integer encoding, where each gene in the chromosome corresponds to a layer's material type and orientation. The integer encoding was used in this research work.

- Fitness Evaluation

Evaluating the fitness of each chromosome is essential to the GA process. The fitness function is designed to reflect the objective function, requiring the analysis of the buckling behavior of each stacking sequence. Chromosomes that violate constraints are penalized through a penalty function, ensuring that only feasible solutions are favored in the selection process.

- Selection

The selection process determines which chromosomes will be used to produce the next generation. Various selection mechanisms can be employed, such as roulette wheel selection, tournament selection, or rank-based selection. These mechanisms typically favor chromosomes with higher fitness values, increasing their chances of being selected as parents for the next generation. The tournament selection type was utilized for this application due to its ability to balance exploration and exploitation, maintain genetic diversity, and handle noisy and multi-modal fitness landscapes.

- Crossover and Mutation

Crossover and mutation are genetic operators that create variability within the population. The crossover operator combines pairs of parent chromosomes to produce offspring, using techniques such as one-point, two-point, or uniform crossover. The crossover rate, which dictates the probability of the occurring crossover, must be carefully selected. The uniform crossover technique was selected for this work because it enhances the exploration of the solution space by promoting high diversity and avoiding premature convergence to local optima. It allows genes to be exchanged between parents with equal probability and ensures thorough mixing of the genetic material, leading to novel and potentially superior stacking sequences. Mutation introduces random changes to individual genes in the offspring chromosomes, with the mutation rate determining the likelihood of these changes. This helps maintain diversity within the population and allows the GA to explore new areas of the search space.

- Replacement and Termination

The replacement step involves creating a new population for the next generation. This was done using elitism, where the best individuals are retained. The GA continues to iterate through selection, crossover, mutation, and replacement until stopping criteria are met. In this case, the termination criterion was reaching the maximum number of generations. After the GA has terminated, the best solution is extracted and analyzed.

4.2. Particle Swarm Optimization

• Problem formulation

To implement Particle Swarm Optimization for stacking-sequence optimization and analysis of buckling in graphene/fiber-reinforced laminated plates, you begin by defining the problem. The objective function needs to be clearly stated, which is to maximize the buckling resistance of the plates while using the minimum amount of expensive nano-reinforcements. The main design variable is the stacking sequences of the laminated plates, where each layer is defined by its material type (e.g., graphene nanoplatelets with carbon or glass fibers) and orientation angle.

• Initialization

The initialization phase involves generating an initial swarm of particles, where each particle represents a potential solution to the stacking-sequence problem. Each particle's position corresponds to a specific stacking sequence, encoded similarly to a chromosome in GA, with material types and orientation angles. The initial velocities of particles are typically set to small random values. This initial population should cover a diverse range of potential solutions to ensure a broad exploration of the search space.

• Fitness Evaluation

The fitness of each particle is evaluated based on the objective function. This evaluation requires analyzing the buckling behavior of each stacking sequence to compute buckling loads. Particles that violate constraints are assigned a lower fitness value or penalized to ensure that the optimization process favors feasible solutions.

• Update Particle Velocities and Positions

The core of PSO lies in updating the velocities and positions of particles based on their own experience and the experience of their neighbors. Each particle's velocity is influenced by three components:

a) **Inertia**: The particle's previous velocity.

b) **Cognitive Component**: The particle's best-known position (personal best).

c) **Social Component**: The best-known position in the swarm (global best).

The velocity update formula is given by,

$$v_i(t+1) = wv_i(t) + c_i r_i\{p_i - x_i(t)\}$$
$$+c_2 r_2\{g - x_i(t)\} \tag{12}$$

where $v_i(t+1)$ is the updated velocity of the particle i, w is the inertia weight, c_1 and c_2 are cognitive and social coefficients, r_1 and r_2 are selected random numbers between 0 and 1, p_i is the personal best position of a particle i, g is the global position found by the swarm, and $x_i(t)$ is the current position of particle i. After updating the velocities, the positions of the particles are updated based on the following equation,

$$x_i(t+1) = x_i(t) + v_i(t+1) \tag{13}$$

• Update Personal and Global Bests

After updating the positions, each particle's fitness is re-evaluated. If a particle's new position yields better fitness than its previous best-known position, the personal best position is updated. Similarly, if any particle's position yields a better fitness than the global best-known position, the global best position is updated.

• Termination

The PSO process iterates through updating velocities, positions, and bests until a stopping criterion is met. The stopping criterion in this study is reaching the maximum number of iterations. Once the algorithm has terminated, the optimal stacking sequence corresponding to the global best position is extracted and analyzed.

5. Numerical Results and Discussions

Numerical results were obtained for two types of fibers, - carbon and glass fibers. The polymer matrix is made of epoxy resin. The laminated plate can also be reinforced with graphene nanoplatelets, and their impact on the buckling was investigated. Material properties for the fibers, matrix, and graphene nanoplatelets are taken from [11] and given next.

Carbon fiber :
$$E_{11} = 263 \text{ GPa}, E_{22} = 19 \text{ GPa},$$
$$G_{12} = 27,6 \text{ GPa}, v_{12} = 0,2 ;$$

Glass fiber :
$$E_{11} = 72,4 \text{ GPa}, E_{22} = 72,4 \text{ GPa},$$
$$G_{12} = 30,2 \text{ GPa}, v_{12} = 0,2 ;$$

Graphene :
$$E_{11} = 1010 \text{ } GPa, E_{22} = 1010 \text{ } GPa,$$
$$G_{12} = 425,8 \text{ } GPa, v_{12} = 0,186 ;$$

Matrix :
$$E_{11} = 3,5 \text{ } GPa, E_{22} = 3,5 \text{ } GPa,$$
$$G_{12} = 1,3 \text{ } GPa, v_{12} = 0,35.$$

The 16-ply laminate in the research paper [5] was taken as a basis for the current analysis. The laminate is balanced and symmetrical and has the following dimensions: a = 1 m, b = 0.5 m, thickness of one ply t = 0.25 mm. Thus, the total plate thickness is $H = 16 \times 0.25 = 4$ mm. Kilonewtons (kN) and kilopascals (kPa) were used to enter the initial data (loads, elastic, and shear moduli). Genetic algorithm (GA) was used for integer optimization and Particle Swarm Optimization (PSO) for the continuous one. All software applications were written by the authors. They are simple yet very fast, accurate, and efficient. The algorithm was tested on the first 12 optimizing problems presented in [5] and the same results were obtained. In this work, only the fiber angles of $0°, \pm45°$, and $90°$ are used.

After that, results were then obtained for carbon-epoxy laminates without nano-inclusions. The optimum stacking sequence was found for different compressive load ratios (N_y/N_x), i.e. different values of load N_y since N_x is assumed to be equal to 1. A standard set of fiber angles of $0°, \pm(15°, 30°, 45°, 60°, 75°)$ and $90°$ is used. The design objective is the maximization of the buckling load for a laminated plate of a given aspect ratio, fiber volume content, GNPs volume fraction, and can be stated as,

$$\lambda_{cr}^{max} \overset{\text{def}}{=} max_\theta \lambda_{cr}(\theta, m, n)$$
$$= max_\theta min_{(m,n)} \lambda_{cr} \tag{14}$$

Although it might not be practical, continuous optimization was also performed where the range of fiber angles for each ply was $\pm(0°, \dots, 90°)$. Such an exercise was done to compare it with the standard approach and check how much improvement can be achieved. The obtained results are presented in Tables 1 and 2. It should be noted that none of these angle sequences are unique, that is, the same optimum critical load can be obtained with a different combination of these fiber angles.

By analyzing the obtained stacking sequence of the fiber angles in Table 1, it can be seen that the fiber orientations for each ply yield. $\pm45°$ when the influence of N_y diminishes. However, with the increase in the ratio N_y to N_x, these angles became equal to $90°$, which is quite obvious. Otherwise, the fiber orientation angles vary between $45°$ and $90°$ but never drop below $45°$. It also should be noted that the number of half waves is $m = 2$ and $n = 1$ for small values of N_y.

The optimization procedure was done based on numerical simulations and by utilizing powerful optimization algorithms. It is difficult to find in the literature experimental findings that tackle the same problem, especially with the inclusion of graphene nanoplatelets. To prove the correctness and efficiency of the optimization procedure, some results obtained in [11] and [19] were successfully repeated.

Table 1. Optimal fiber sequence in carbon-epoxy laminate

N_y/N_x	Integer optimization	λ_{cr}	Continuous optimization	λ_{cr}	m,n
0.125	$(45_2°/-45°/45_2°/-45_2°/45°)_S$	105.86	[SAME]		2,1
0.25	$(45_2°/60°/-60°/60_2°/-45°/90°)_S$	92.40	$(-52_2°/52°/-52_3°/52_2°)_S$	93.85	2,1
0.5	$(60_3°/-75°/-60°/-75°/60°/-60°)_S$	71.95	$(62_2°/-62°/62°/-62_3°/68°)_S$	72.06	1,1
1.0	$(-75_2°/75_2°/60°/-75°/60°/-75°)_S$	47.28	$(74°/-74°/74°/-74°/74_3°/-74°)_S$	47.57	1,1
1.5	$(90_2°/-75°/75°/90°/-75_3°)_S$	34.97	$(81_3°/-81°/82_2°/81°/-81°)_S$	34.99	1,1
2.0	$(90_8°)_S$	27.85	[SAME]		1,1
3.0	$(90_8°)_S$	19.08	[SAME]		1,1

Table 2. Optimal fiber sequence in glass-epoxy laminate

N_y/N_x	Integer and continuous optimization	λ_{cr}	m,n
0.125	$(90_3°/0°/90_2°/0_2°)_S$	56.46	2,1
0.25	$(90_2°/0_2°/90_2°/0_2°)_S$	49.62	2,1
0.5	$(90°/0_2°/90°/0°/90_2°/0°)_S$	33.08	1,1
1.0	$(0°/90_3°/0°/90°/0_2°)_S$	19.85	1,1
1.5	$(90°/0_2°/90_3°/0_2°)_S$	14.18	1,1
2.0	$(0_2°/90°/0°/90_3°/0°)_S$	11.03	1,1
3.0	$(90°/0_2°/90°/0°/90_2°/0°)_S$	7.63	1,1

The continuous optimization demonstrates to us that the use of the entire set of angles is unfeasible to be of practical use since the increase in the critical buckling load is negligible.

The glass fibers exhibit a different pattern of behavior, as seen in Table 2. Here only the angles of $0°$ and $90°$, independently of the ratio (N_y/N_x), form the stacking sequence. Moreover, continuous optimization produces absolutely the same results. Such results can be attributed to the isotropic nature of the glass fibers.
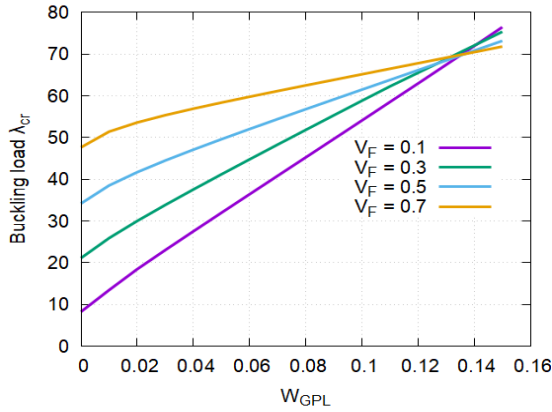
Fig. 2. Buckling load versus weight fraction of graphene for carbon fiber reinforced laminate with different values of the fiber volume content ($N_y/N_x = 0.5$)
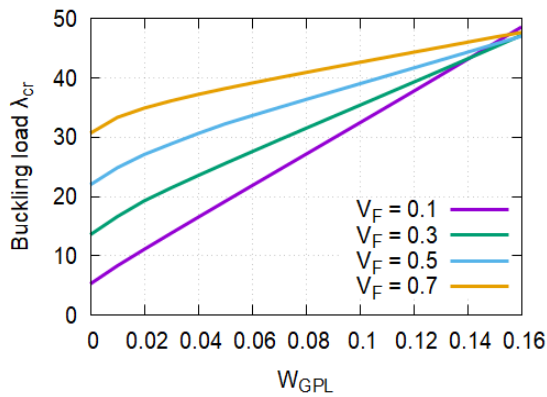
Fig. 3. Buckling load versus weight fraction of graphene for carbon fiber reinforced laminate with different values of the fiber volume content ($N_y/N_x = 1$)
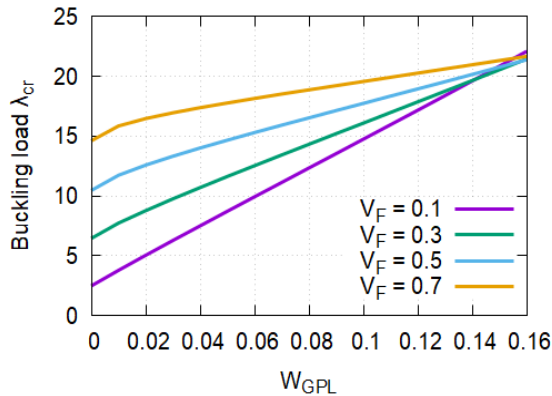
Fig. 4. Buckling load versus weight fraction of graphene for carbon fiber reinforced laminate with different values of the fiber volume content ($N_y/N_x = 2.5$)
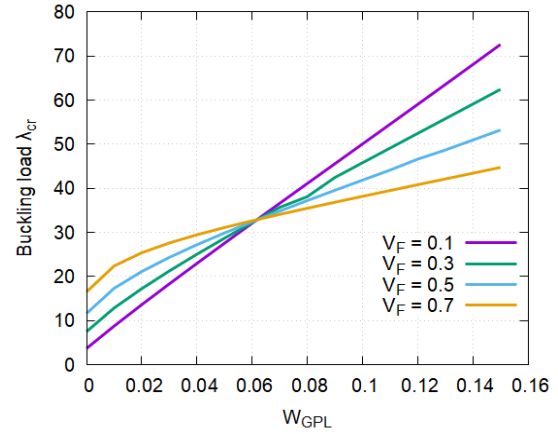
Fig. 5. Buckling load versus weight fraction of graphene for glass fiber reinforced laminate with different values of the fiber volume content ($N_y/N_x = 0.5$)
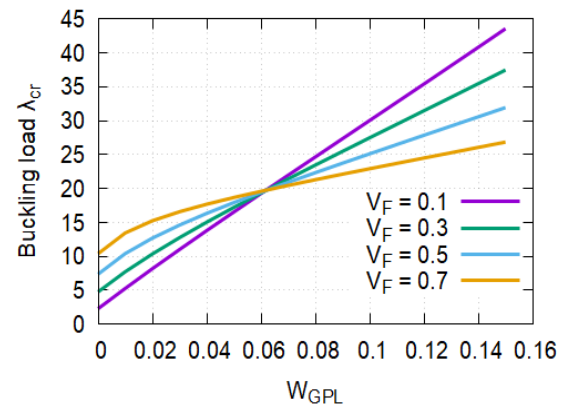
Fig. 6. Buckling load versus weight fraction of graphene for glass fiber reinforced laminate with different values of the fiber volume content ($N_y/N_x = 1$)
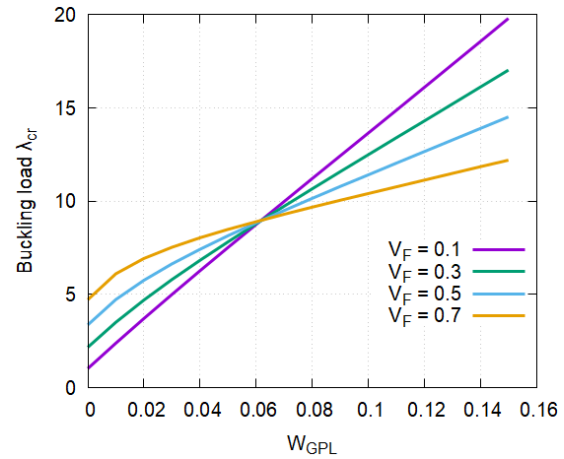
Fig. 7. Buckling load versus weight fraction of graphene for glass fiber reinforced laminate with different values of the fiber volume content ($N_y/N_x = 2.5$)

Next, we investigate the effect of the reinforcement of graphene nanoplatelets on the buckling load. For this purpose, we considered three (N_y/N_x) ratios of 0.5, 1.0, and 2.5, and both types of fiber reinforcement, carbon and glass fibers. Four different fiber volume content quantities V_F were considered, namely, 0.1, 0.3, 0.5, and 0.7.

Figures 2, 3, and 4 show the influence of the amount of graphene, i.e., its weight fraction on the critical buckling load for different values of carbon fiber volume content. As expected, the buckling load increases along with the increase in fiber volume content. However, the higher the fiber volume content, the slower the rate of increase of the buckling load with the increase of the weight fraction of graphene. Such behavior results in a crossover point where the buckling load becomes the same for all the values of the fiber content. This interesting phenomenon was shown and described in [11] for sandwich plates with a soft core. For load ratio $N_y/N_x = 0.5$ this point is distinct and corresponds to $W_{GPL} = 0.134$. But in the case of the load ratio being equal to 1.0 and 2.5, we can see a few crossover points located in the region of approximately. $W_{GPL} = 0.14, \cdots, 0.17$. As pointed out in [11], such results are because of the contribution of Young's modulus of the graphene-reinforced matrix E_{GM} in Eq. (5) decreases as the fiber content increases and the contribution of E_{GM} to E_{11} also decreases, as can be seen in Eq. (8). This effect was also demonstrated experimentally in [17] and tells us that the high graphene content should be avoided.

The performance of the glass fiber reinforced plate shown in Figures 5, 6, and 7 is somewhat different due to its isotropic nature. The crossover point in all cases of the load ratios is located at the same place, calculated at $W_{GPL} = 0.063$. Interestingly, it is the same value as obtained in [11] for different aspect ratios of a/b. Thus, the above results help us to properly balance the content values of fibers and nano-reinforcements to produce cost-effective designs. In the case of carbon fiber reinforcement, the upper limit of graphene content should not exceed 10%, while in the case of glass fibers, it should be twice less, i.e., less than 5%. These revelations help to understand the graphene content limits when designing graphene/fiber-reinforced laminates. Exceeding the limits leads to using excessive and expensive nano-reinforcements but with no increase in the buckling resistance of the nanocomposite laminate. Therefore, for designing cost-effective laminated plates under the same loading conditions and using glass or carbon fibers, the given graphene content limits should be maintained.

Figures 8 and 9 illustrate the three-dimensional plot of buckling load concerning graphene weight and fiber volume content for both carbon and glass laminates. It can be seen that the change in the buckling load is generally smooth in both cases. The extreme points, however, result in sharp changes in the critical

load, specifically where one of the parameters is zero and the buckling load fully depends only on the fibers or the graphene nanoplatelets.
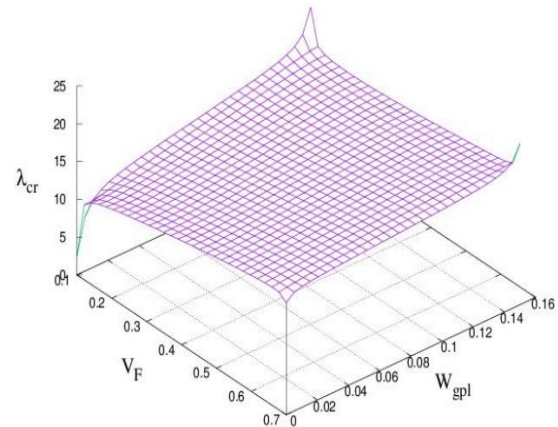
Fig. 8. The buckling load versus the values of graphene weight and fiber volume content (carbon fibers)
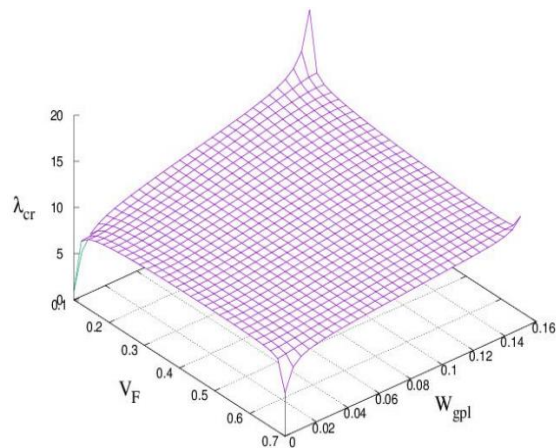
Fig. 9. The buckling load versus the values of graphene weight and fiber volume content (glass fibers)

6. Limitations, Future Work, and Recommendations.

Using the GA and PSO for optimizing the stacking sequence of graphene/fiber-reinforced laminated plates has significant practical implications, particularly in enhancing structural performance. By optimizing the stacking sequence, these algorithms can identify configurations that maximize buckling resistance, leading to stronger and more resilient structures. However, the use of GA and PSO is not without limitations. One of the primary challenges is the high computational cost associated with these algorithms. Both GA and PSO can be computationally intensive, especially when dealing with large-scale problems involving many design variables, such as numerous layers in a laminate. This can lead to long optimization times and require significant computational resources, which may be a limitation in practical applications.

To further improve the outcomes of this research, exploring more advanced or hybrid evolutionary algorithms could be beneficial. For instance, combining evolutionary algorithms with machine learning techniques might enhance the convergence speed and solution quality, making the optimization process more efficient. Developing specialized software tools that integrate optimization and analysis processes is also recommended, as this would make the approach more accessible to engineers and researchers working in the field.

In future research, the proposed optimization and buckling analysis techniques can also be extended to other advanced composite materials or hybrid systems. This could involve exploring materials with different properties or combinations, such as carbon nanotubes or boron nitride, which may offer unique advantages in specific applications. Additionally, the use of 3D elasticity theories or higher-order shear deformation theories could be investigated to improve the accuracy of buckling analysis, especially for thicker laminated plates where traditional 2D models may fall short.

Another area of exploration could be the extension of this work to a multi-objective optimization framework. In this context, other structural performance criteria such as vibration, thermal stability, or impact resistance could be considered alongside buckling, providing a more comprehensive design optimization.

7. Concluding Remarks

The problem of the optimum stacking sequence and structural performance of laminated composite simply supported plates subject to biaxial compressive buckling load was addressed in this study. By applying the optimization procedure, the optimum orientation was obtained for different load ratios. Both two- and three-phase laminates reinforced with carbon or glass fibers and graphene nanoplatelets were considered. A cost-effective design using the minimum amount of expensive reinforcement while maximizing the compressive buckling load was proposed. The difference between carbon and glass fiber reinforcement, which manifests in the behavior of the laminates because of the different nature of the material properties, was highlighted. The obtained results are useful for properly balancing the content values of the fibers and graphene nanoplatelets in the design of laminated composite plates. In the case of carbon fiber reinforcement, the upper limit of graphene content should not exceed 10%, while in the case of glass fibers, it should be twice less, i.e., less than 5%. The obtained results are of obvious interest to engineers and researchers alike.

Conflicts of Interest

The author declares that there is no conflict of interest regarding the publication of this article.

References

[1] Fu, S.Y., Lauke, B. and Mai, Y.W., 2009. *Science and Engineering of Short Fiber-Reinforced Polymer Composites*. Woodhead Publishing.

[2] Parveen, S., Rana, S. and Fangueiro, R., 2017. *Advanced Composite Materials: Properties and Applications*. De Gruyter Brill.

[3] Rafiee, M., Nitzsche, F. and Labrosse, M., 2018. Modeling and mechanical analysis of multiscale fiber-reinforced graphene composites: Nonlinear bending, thermal post-buckling and large amplitude vibration. *International Journal of Non-Linear Mechanics*, *103*(1), pp.104-112. doi.org/10.1016/j.ijnonlinmec.2018.05.004.

[4] Rafiee, M.A., Rafiee, J., Wang, Z., Song, H., Yu, Z.Z. and Koratkar, N., 2009. Enhanced mechanical properties of nanocomposites at low graphene content. *ACS Nano*, *3*(12), pp.3884-3890. doi.org/10.1021/nn9010472.

[5] Kim, H., Abdala, A.A. and Macosko, C. W., 2010. Graphene/polymer nanocomposites. *Macromolecules*, *43*(16), pp.6515-6530. doi.org/10.1021/ma100572e.

[6] Safaei, B. and Fattahi, A., 2017. Free vibrational response of single-layered graphene sheets embedded in an elastic matrix using different non-local plate models. *Mechanics*, *23*(5), pp.678-687. doi.org/10.5755/j01.mech.23.5.14883.

[7] Su, X., Wang, R., Li, X., Araby, S., Kuan, H.C., Naeem, M. and Ma, J., 2022. A comparative study of polymer nanocomposites containing multi-walled carbon nanotubes and graphene nanoplatelets. *Nano Materials Science*, *4*(3), pp.185-204. doi.org/10.1016/j.nanoms.2021.08.003.

[8] Shokrieh, M., Ghoreishi, S., Esmkhani, M. and Zhao, Z., 2014. Effects of graphene nanoplatelets and graphene nanosheets on fracture toughness of epoxy nanocomposites. *Fatigue & Fracture of Engineering Materials & Structures*, *37*(10), pp.1116-1123. doi.org/10.1111/ffe.12191.

[9] Ebrahimi, F. and Dabbagh, A., 2021. An analytical solution for static stability of multi-scale hybrid nanocomposite plates. *Engineering with Computers*, *37*(1), pp.545-559. doi.org/10.1007/s00366-019-00840-y.

[10] Song, M., Yang, J., Kitipornchai, S. and Zhu W., 2017. Buckling and post-buckling of biaxially compressed functionally graded multilayer graphene nanoplatelet-reinforced polymer composite plates. *International Journal of Mechanical Sciences*, *131*(1), pp.345-355. doi.org/10.1016/j.ijmecsci.2017.07.017.

[11] Radebe, I.S., Drosopoulos, G.A. and Adali, S., 2019. Buckling of non-uniformly distributed graphene and fiber-reinforced multiscale angle-ply laminates. *Meccanica*, *54*(14), pp. 2263-2279. doi.org/10.1007/s11012-019-01067-3.

[12] Radebe, I.S., Drosopoulos, G.A. and Adali, S., 2022. Effect of Non-Uniform Fiber Distribution along Thickness and Non-Uniform Ply Thicknesses on Frequencies of Symmetric Angle-Ply Laminates. *Fibers and Polymers*, *23*(8), pp.2250-2260. doi.org/10.1007/s12221-022-4440-5.

[13] Georgantzinos, S.K., Giannopoulos, G. I. and Markolefas, S. I., 2020. Vibration analysis of carbon fiber-graphene-reinforced hybrid polymer composites using finite element techniques. *Materials*, *13*(19), p.4225. doi.org/10.3390/ma13194225.

[14] Jeawon, Y., Drosopoulos, G., Foutsitzi, G., Stavroulakis, G. and Adali, S., 2021. Optimization and analysis of frequencies of multi-scale graphene/fiber reinforced nanocomposite laminates with non-uniform distributions of reinforcements. *Engineering Structures*, *228*(2). p.111525. doi.org/10.1016/j.engstruct.2020.111525.

[15] Chao, C., Koh, S. and Sun, C., 1975. Optimization of buckling and yield strengths of laminated composites. *AIAA Journal*, *13*(9), pp.1131-1132. doi.org/10.2514/3.60515.

[16] Chen, T.L., 1976. Design of composite-material plates for maximum uniaxial compressive buckling load. *Proceedings of the Oklahoma Academy of Science*, *56* (1976), pp.104-107.

[17] Schmit Jr, L. and Farshi, B., 1977. Optimum design of laminated fiber composite plates. *International Journal for Numerical Methods in Engineering*, *11*(4), pp.623-640, doi.org/10.1002/nme.1620110403.

[18] Hirano, Y., 1979. Optimum design of laminated plates under axial compression. *AIAA Journal*, *17*(9), pp.1017-1019. doi.org/10.2514/3.61269.

[19] Haftka, R.T. and Walsh, J.L., 1992. Stacking-sequence optimization for buckling of laminated plates by integer programming. *AIAA Journal*, *30*(3), pp.814-819. doi.org/10.2514/3.10989.

[20] Chai, G. and Hoon, K., 1992. Buckling of generally laminated composite plates. *Composites Science and Technology,* *45*(2), pp.125-133. doi.org/10.1016/0266-3538(92)90035-2.

[21] Kicher, T. and Mandell, J., 1971. A study of the buckling of laminated composite plates. *AIAA Journal*, *9*(4), pp.605-613. doi.org/10.2514/3.6237.

[22] Chattopadhyay, A. and Gu, H., 1994. New higher-order plate theory in modeling delamination buckling of composite laminates. *AIAA Journal*, *32*(8), pp.1709-1716. doi.org/10.2514/3.12163.

[23] Jane, K., Liao, H. and Hong, W., 2003. Validation of the Rayleigh–Ritz method for the post-buckling analysis of rectangular plates with application to delamination growth. *Mechanics Research Communications*, *30*(6), pp.531-538. doi.org/10.1016/S00936413(03)00060-0.

[24] Darvizeh, M., Darvizeh, A., Ansari, R. and Sharma, C., 2004. Buckling analysis of generally laminated composite plates (generalized differential quadrature rules versus Rayleigh–Ritz method). *Composite Structures*, *63*(1), pp.69-74. doi.org/10.1016/S0263-8223(03)00133-8.

[25] Karakaya, Ş. and Soykasap, Ö., 2009. Buckling optimization of laminated composite plates using genetic algorithm and generalized pattern search algorithm. *Structural and Multidisciplinary Optimization*, *39*(3), pp.477-486. doi.org/10.1007/s00158-008-0344-2.

[26] Nikbakt, S., Kamarian, S. and Shakeri, M., 2018. A review on optimization of composite structures Part I: Laminated composites. *Composite Structures*, *195*(1), pp.158-185. doi.org/10.1016/j.compstruct.2018.03.063.

[27] Vosoughi, A., Darabi, A., Anjabin, N. and Topal, U., 2017. A mixed finite element and improved genetic algorithm method for maximizing buckling load of stiffened laminated composite plates. *Aerospace Science and Technology*, *70*(4), pp.378-387. doi.org/10.1016/j.ast.2017.08.022.

[28] Keshtegar, B., Nguyen-Thoi, T., Truong, T.T. and Zhu, S.P., 2021. Optimization of buckling load for laminated composite plates using adaptive Kriging-improved PSO: A novel hybrid intelligent method. *Defense Technology*, *17*(1), pp.85-99. doi.org/10.1016/j.dt.2020.02.020.

[29] Kaveh, A., Dadras, A. and Malek, N.G., 2019. Optimum stacking sequence design of composite laminates for maximum buckling load capacity using parameter-less optimization algorithms. *Engineering with Computers*, *35*(1), pp.813-832. doi.org/10.1007/s00366-018-0634-2.

[30] Fakoor, M., Ghoreishi, S.M.N. and Aminjafari, M., 2019. Multi-objective optimization of buckling load for a laminated composite plate by coupling genetic algorithm and FEM. *Journal of Aerospace Science and Technology*, *12*(1), pp.27-37.

[31] Leissa, A.W., 1987. A review of laminated composite plate buckling. *Applied Mechanics Reviews*, *40*(5), pp. 575-591. doi.org/10.1115/1.3149534.

[32] Baba, B.O., 2007. Buckling behavior of laminated composite plates. *Journal of Reinforced Plastics and Composites*, *26*(16), pp.1637-1655. doi.org/10.1177/0731684407079515.

[33] El-Sawy, K.M. and Nazmy, A.S., 2001. Effect of aspect ratio on the elastic buckling of uniaxially loaded plates with eccentric holes. *Thin-Walled Structures*, *39*(12), pp.983-998. doi.org/10.1016/S0263-8231(01)00040-4.

[34] Soden, P.D., Hinton, M.J. and Kaddour, A., 1998. Lamina properties, lay-up configurations, and loading conditions for a range of fiber reinforced composite laminates. *Failure Criteria in Fiber-Reinforced-Polymer Composites: Elsevier*, *58*(17) pp.1011-1022. doi.org/10.1016/S0266-3538(98)00078-5.

[35] Ren, J., 2021. *Handbook of Ceramics and Composites.* CRC Press.

[36] Aslan, Z. and Şahin, M., 2009. Buckling behavior and compressive failure of composite laminates containing multiple large delaminations. *Composite Structures*, *89*(3), pp.382-390. doi.org/10.1016/j.compstruct.2008.08.011.

[37] Vosoughi, A., Darabi, A. and Forkhorji, H.D., 2017. Optimum stacking sequences of thick laminated composite plates for maximizing buckling load using FE-GAs-PSO. *Composite Structures*, *159*(1), pp.361-367. doi.org/10.1016/j.compstruct.2016.09.085.

[38] Ehsani, A. and Rezaeepazhand, J., 2016. Stacking sequence optimization of laminated composite grid plates for maximum buckling load using genetic algorithm. *International Journal of Mechanical Sciences*, *119*(1), pp.97-106. doi.org/10.1016/j.ijmecsci.2016.09.028.

[39] Chen, Q. and Qiao, P., 2021. Buckling and post-buckling of rotationally restrained laminated composite plates under shear. *Thin-Walled Structures*, *161*(1), p.107435. doi.org/10.1016/j.tws.2021.107435.

[40] Bert, C.W. and Malik, M., 1997. On the buckling characteristics of symmetrically laminated cross-ply plates. *Mechanics of Composite Materials and Structures*, *4*(1), pp. 39-67. doi.org/10.1080/10759419708945874.

[41] Weaver, P.M. and Nemeth, M.P., 2007. Bounds on flexural properties and buckling response for symmetrically laminated composite plates. *Journal of Engineering Mechanics*, *133*(11), pp.1178-1191. doi.org/10.1061/(ASCE)07339399(2007)133:11(1178).